Momentum alignment and spin orientation of photoexcited electrons in quantum wells

I. A. Merkulov, V. I. Perel', and M. E. Portnoi

A. F. Ioffe Physicotechnical Institute, USSR Academy of Sciences, Leningrad

(Submitted 1 June 1990)
Zh. Eksp. Teor. Fiz. 99, 1202–1214 (April 1991)

We have calculated the distribution function with respect to momentum and spin of photoexcited electrons in a quantum well with infinitely high walls pumped by polarized light incident normal to the plane of the heterostructure. When the ratio of light- to heavy-hole masses is small, an anomalously rapid increase in the momentum alignment takes place along with a decrease in the orientation of electron spins with increasing energy of electron motion in the plane of the well. We find the dependence on excitation photon energy of the linear and circularly-polarized hot luminescence in the direction of pumping near its short-wavelength edge.

In bulk semiconductors of GaAs type, electrons that are created via interband absorption of linearly polarized light are aligned with respect to momentum,[1-3] while excitation by circularly polarized light results in orientation of the electron spins.[3] Optical spin orientation of the electrons leads to circularly polarized recombination radiation, while alignment of their momenta is manifest in linear polarization of the hot photoluminescence. Circular polarization of edge luminescence from optically-pumped quantum wells has been observed as well.[4,5] The corresponding theory was developed in Refs. 4–6, while orientation and alignment effects in the polarization of hot luminescence from quantum wells were recently seen in experiments.[7]

In this paper we find the distribution function for photoexcited electrons in a quantum well with respect to momentum and spin. In order to reveal the fundamental regularities of the alignment and orientation effects, we will discuss the simplest case of an infinitely deep symmetric well, ignoring the absence of a center of inversion in crystals of GaAs type. The degree of anisotropy in the distribution function of the photoexcited electrons depends considerably on the energy of the excitation photons. This dependence is quite abrupt compared to the three-dimensional case, especially when the ratio of the masses of light and heavy holes (m_l/m_h) is small, and is associated with an abrupt restructuring of the hole wave function for values of the two-dimensional wave vector $k \simeq (m_l/m_h)^{1/2}/L$, where L is the width of the well. This change in the wave function also affects the spectral functions for linearly- and circularly-polarized hot photoluminescence. We note that structure in the absorption coefficient of superlattices based on GaAs was observed at anomalously small wave vector values of the photoexcited electrons in the numerical calculations described in Ref. 8.

1. The four Bloch states of an electron in the heavy and light hole bands are described by the wave functions

$$\psi_{kq}^{(M)} = \exp(i\mathbf{k}\boldsymbol{\rho})\exp(iq_M z)\, u_{kq_M}^{(M)}(\mathbf{r}). \tag{1}$$

Here $u_{kq_M}^{(M)}(r)$ is the Bloch amplitude; M labels the four states (in the spherical model M can denote helicity). The z-axis is directed along the normal to the plane of the well; in what follows, we will assume that it coincides with the direction [001]. k is the wave vector in the plane of the well. If the values of energy E and wave vector k are fixed, then the value of q must satisfy the equation

$$\varepsilon^2 - 2\gamma_1\varepsilon(q^2+k^2) + (\gamma_1^2 - 4\gamma_2^2)(k^2+q^2)^2 - 12\gamma\gamma_2^2(k_x^2k_y^2 + q^2k^2) = 0, \tag{2}$$

where

$$\varepsilon = 2m_0E/\hbar^2, \quad \gamma = (\gamma_3^2-\gamma_2^2)/\gamma_2^2,$$

and $\gamma_1, \gamma_2, \gamma_3$ are the Luttinger parameters. Equation (2) is satisfied by two values of q^2 which correspond to heavy and light holes in the spherical approximation. When warping of the energy surfaces is taken into account it can turn out that both values of q^2 correspond to heavy holes.[1)] Nevertheless, we will use the notation $q_1 = q_2 = q_h$, $q_3 = q_4 = q_l$ ($q_h^2 > q_l^2$). The Bloch amplitudes u_{kq} can be written in the form

$$u_{kq}^{(M)} = \sum_{\mu} u_{\mu}(\mathbf{r})\,\chi_{\mu}^{(M)}(\mathbf{k}, q),$$

where u_μ are the four degenerate states of the top of the valence band:

$$u_{\pm 3/2} = \mp\frac{1}{2^{1/2}}(X \pm iY)s_{\pm},$$

$$u_{\pm 1/2} = \frac{1}{3^{1/2}}\left[\mp\frac{1}{2^{1/2}}(X \pm iY)s_{\mp} + 2^{1/2}Zs_{\pm}\right];$$

here $s_\pm$ are spin functions corresponding to directions along the z-axis and opposite to it.

The components $(\chi_{3/2}, \chi_{1/2}, \chi_{-1/2}, \chi_{-3/2})$ can be found by the Hopfield method:

$$\chi^{(1)} = (q_h a^*,\ b_h,\ 0,\ c), \quad \chi^{(2)} = (-c^*,\ 0,\ -b_h,\ q_h a),$$
$$\chi^{(3)} = (q_l a^*,\ b_l,\ 0,\ c), \quad \chi^{(4)} = (-c^*,\ 0,\ -b_l,\ q_l a),$$
$$a = 2\cdot 3^{1/2}\gamma_3(k_x - ik_y), \quad c = 3^{1/2}[\gamma_3(k_x^2 - k_y^2) + 2i\gamma_3 k_x k_y],$$
$$b_h = (\gamma_1+\gamma_2)k^2 + (\gamma_1 - 2\gamma_2)q_h^2 - \varepsilon,$$
$$b_l = (\gamma_1+\gamma_2)k^2 + (\gamma_1 - 2\gamma_2)q_l^2 - \varepsilon. \tag{3}$$

In the calculations that follow it is convenient to introduce the notation

$$b_h/(3^{1/2}|c|) = \tilde{p}, \quad c/(q_h a) = \tilde{s}.$$

2. Let us construct the states of the symmetric quantum well out of combinations of the functions (1) that are sym-

 0038-5646/91/040669-07$03.00

metric or antisymmetric with respect to the plane $z=0$, which is assumed to pass through the center of the well. The symmetric combination can be written in the form

$$\psi_s^{(M)}=1/2(1+\hat{\Pi})\psi_{k\varphi,M}, \tag{4}$$

where $\hat{\Pi}$ is the operator for reflection in the plane $z=0$; when spin is included, $\hat{\Pi}$ is defined by the equation $\hat{\Pi}\psi(z)=\hat{\sigma}_z\psi(-z)$.

In a symmetric well two states belong to each energy level: a symmetric state and an antisymmetric state. It is natural to seek the symmetric functions in the form of linear combinations of the functions (4):

$$\Psi_s=\sum_M A_M\psi_s^{(M)}. \tag{5}$$

The antisymmetric function can be obtained by applying successively the operations of inversion $\hat{J}$ and time reversal $\hat{K}$ to (5) (where $\hat{K}\psi=-i\hat{\sigma}_y\psi^*$; see Ref. 9):

$$\Psi_a=\hat{J}\hat{K}\Psi_s. \tag{6}$$

The Bloch amplitudes $u_{3/2}$, $u_{-1/2}$ are symmetric, while $u_{1/2}$, $u_{-3/2}$ are antisymmetric with respect to the operation $\hat{\Pi}$; therefore, the symmetric functions (4) (which are unnormalized) have the form

$$\psi_s^{(M)}=e^{ikr}\{[\chi_{3/2}^{(M)}u_{3/2}+\chi_{-1/2}^{(M)}u_{-1/2}]\cos(q_Mz)$$

$$+i[\chi_{1/2}^{(M)}u_{1/2}+\chi_{-3/2}^{(M)}u_{-3/2}]\sin(q_Mz)\}. \tag{7}$$

3. For an infinitely deep rectangular well the boundary conditions for the functions Ψ_s consist of setting the envelopes equal to zero at the walls of the well (i.e., $z=\pm L/2$; in what follows the quantity $L/2$ will be taken to have unit length). This condition is conveniently written in the form

$$\sum_{M=3,4}A_M\chi_\mu^{(M)}=-\sum_{M=1,2}A_M\chi_\mu^{(M)}\zeta_\mu,\quad \mu=3/2,\ 1/2,\ -1/2,\ -3/2, \tag{8}$$

where $\zeta_\mu=c_h/c_l$ for $\mu=3/2,\ -1/2$ and $\zeta_\mu=s_h/s_l$ for $\mu=1/2,\ -3/2$. Here and in what follows we use the notation

$$c_l=\cos q_l,\quad c_h=\cos q_h,\quad s_l=\sin q_l,\quad s_h=\sin q_h.$$

Introducing the explicit form of $\chi^{(M)}$, using Eq. (8) we can express A_3 and A_4 in terms of A_1 and A_2 and obtain the ratio between A_1 and A_2:

$$A_3=-\frac{s_hb_h}{s_lb_l}A_1,\quad A_4=-\frac{c_hb_h}{c_lb_l}A_2,\quad \frac{A_1}{A_2}=v\xi^*, \tag{9}$$

where v is a real quantity; using either of the two equations

$$v=\frac{b_l-b_h}{b_l-b_h\tau}=q_h^2\left|\frac{a}{c}\right|^2\frac{(b_hq_l^2/q_h^2\tau)-b_l}{b_l-b_h}, \tag{10}$$

v can be expressed in terms of the variable

$$\tau=q_l\operatorname{tg}q_h/q_h\operatorname{tg}q_l. \tag{11}$$

The second of Eqs. (10) leads to a quadratic equation for τ:

$$\tau^2+2\Phi\tau+q_l^2/q_h^2=0,$$

$$-2\Phi=\frac{b_l}{b_h}|\xi|^2\left(1-\frac{b_h}{b_l}\right)^2+\frac{b_hq_l^2}{b_lq_h^2}+\frac{b_l}{b_h}. \tag{12}$$

Equations (11) and (12) together with Eq. (2) determine the values of q_h and q_l for a given k and thereby the energy spectrum in the size quantization band. The equations for the spectrum were obtained previously by Nedorezov.[10]

The wave function can be written in the following form, which is convenient for further calculations:

$$\Psi_s=Ne^{ikr}[-(u_{3/2}+3^{1/2}W_+u_{-3/2})C(z)+i\eta(u_{-3/2}+3^{1/2}W_-u_{3/2})S(z)], \tag{13}$$

where

$$C(z)=\cos(q_hz)-(c_h/c_l)\cos(q_lz),$$
$$S(z)=\sin(q_hz)-(s_h/s_l)\sin(q_lz), \tag{14}$$

$$W_+=W_+\exp(2i\varphi_k),\quad W_-=W_-\exp(-2i\varphi_k),$$

$$W_+=\frac{\beta}{1-v},$$

$$W_-=\beta\left[1+\frac{1}{|\xi|^2v}\right]^{-1},\quad \eta=\frac{v\xi^*W_+}{W_-},$$

$$|\eta|^2=\frac{W_+(W_+-\beta)}{W_-(\beta-W_-)}.$$

The angle φ_k is determined by the relation $c=|c|\exp(2i\varphi_k)$.

Let us note the following fact: Eq. (12) has two solutions

$$\tau_{1,2}=-[\Phi\pm(\Phi^2-q_l^2/q_h^2)^{1/2}]. \tag{15}$$

Solution τ_1 [the upper sign in Eq. (15)] corresponds to subbands of heavy holes with odd indices and light holes with even indices, while solution τ_2 is associated with the remaining subbands. (The enumeration and terminology of the subbands is based on energy values at $k=0$.) The values of τ_1 and τ_2 are connected by the ratio $\tau_1\tau_2=q_l^2/q_h^2$. From Eq. (10), which expresses v in terms of τ, for fixed k and q_h we can obtain

$$v_1v_2=-1/|\xi|^2.$$

From this and from Eq. (14) we find the following relations (for fixed k, q_h, q_l)

$$(W_\pm)_2=(W_\mp)_1,\quad \eta_1\eta_2^*=-1. \tag{16}$$

The constant N is determined from the normalization conditions:

$$N=[(1+3W_+^2)\mathscr{P}_c+|\eta|^2(1+3W_-^2)\mathscr{P}_s]^{-1},$$

$$\mathscr{P}_c=\left(1+\frac{c_h^2}{c_l^2}\right)+\frac{c_h}{c_l}\frac{s_hc_l(q_l^2+3q_h^2)q_l-s_lc_h(q_h^2+3q_l^2)q_h}{q_lq_h(q_l^2-q_h^2)},$$

$$\mathscr{P}_s=\left(1+\frac{s_h^2}{s_l^2}\right)+\frac{s_h}{s_l}\frac{s_hc_l(q_h^2+3q_l^2)q_h-s_lc_h(q_l^2+3q_h^2)q_l}{q_lq_h(q_l^2-q_h^2)}. \tag{17}$$

4. All these expressions simplify greatly in the spherical approximation ($\gamma_3=\gamma_2$). For this case $\beta=1$,

$\xi = (k/2q_h)\exp(2i\varphi_k)$, and φ_k reduces to the angle between the vector k and the x-axis. From Eq. (2) it now follows that

$$\varepsilon = \frac{m_0}{m_h}(k^2+q_h^2) = \frac{m_0}{m_l}(k^2+q_l^2), \tag{18}$$

where m_l and m_h are the effective masses of light and heavy holes, and Eqs. (12) and (15) coincide with the equations obtained previously by D'yakonov and Khaetskii;[11] in these equations,

$$\Phi = \frac{6t^2-3t-3\nu t+4\nu}{6t(1-t)}, \quad \frac{q_l^2}{q_h^2} = \frac{\nu-t}{1-t}. \tag{19}$$

Here we have introduced the variable $t = k^2/(k^2+q_h^2)$ and the notation $\nu = m_l/m_h$. We note that for $t > \nu$ the quantity q_l is pure imaginary.

The parameters $W_\pm$, $|\eta|^2$, and τ are completely determined by the value of the variable t. For these quantities we obtain the following expressions:

$$(W_\mp)_1 = (W_\pm)_1 = \frac{\nu+1}{2}\left\{\left(1-\frac{t_0}{t}\right) \pm \left[\left(1-\frac{t_0}{t}\right)^2 + \frac{t_0}{1+\nu}\right]^{1/2}\right\},$$

$$t_0 = \frac{4\nu}{3(1+\nu)}$$

$$|\eta|^2 = \frac{W_+(1-W_+)}{W_-(W_--1)}, \quad \tau = \frac{W_--t}{1-t}. \tag{20}$$

We note that for small mass ratios the wave functions undergo abrupt changes in the small-k region ($t \approx t_0$).

For $t \gg t_0$ ($t_0 \ll 1$) the wave functions do not depend on the mass ratio: for states of type 1,

$$(W_+)_1 \approx 1, \quad (W_-)_1 \approx 0, \quad |\eta|_1^2 \approx (1-t)/t, \quad \tau_1 \approx -t/(1-t), \tag{21}$$

and for states of type 2,

$$(W_+)_2 \approx 0, \quad (W_-)_2 \approx 1, \quad |\eta|_2^2 \approx t/4(1-t), \quad \tau_2 \approx 1. \tag{22}$$

For energy levels that are not too high, as long as νq_h, νq_l are small the quantities q_h and q_l themselves, which are determined from Eq. (11), are independent of ν, since we can set $q_l^2 \approx -q_h^2 t/(1-t)$ in this equation. In this case

$$\mathcal{P}_{e1} \approx 1 + \frac{c_h^2}{c_l^2} - \frac{s_h c_h}{q_h}\frac{1-2t}{t}, \quad \mathcal{P}_{s1} \approx 1 + \frac{s_h^2}{s_l^2} + 2\frac{s_h c_h}{q_h},$$

$$\mathcal{P}_{e2} \approx 1 + \frac{c_h^2}{c_l^2} - 2\frac{s_h c_h}{q_h}, \quad \mathcal{P}_{s2} \approx 1 + \frac{s_h^2}{s_l^2} + \frac{s_h c_h}{q_h}\frac{1-2t}{t}. \tag{23}$$

5. Let us turn to a calculation of the distribution function for the photoexcited electrons. The wave functions in the conduction band that are symmetric with respect to reflection in the plane $z = 0$ are as follows:

$$\Phi_s^+ = Se^{ikp}\cos(p_+ z)s_+, \quad \Phi_s^- = Se^{ikp}\sin(p_- z)s_-, \tag{24}$$

where S is the Bloch amplitude of S type, $p_+ = (2n+1)\pi/2$, and $p_- = n\pi$. The functions Φ_s^+ and Φ_s^- possess coordinate parts with different symmetries, but when the spin parts are included both are symmetric. Two states, symmetric and antisymmetric, correspond to each energy level in the conduction band (just as in the valence band). The antisymmetric states are obtained from (24) by the operator $\hat{J}\hat{K}$; although they are characterized by the same values of p_+ and p_-, the spin direction of the even function is "down" while that of the odd function is "up".

Dipole optical transitions induced by excitation light with its electric vector lying in the xy plane are allowed only between states of the same symmetry. Therefore, the density matrix of photoexcited electrons is diagonal. In the electron subband with odd label the distribution functions for electrons with up and down spin are given by the following expression (with a constant factor):

$$\mathcal{F}_\uparrow = \rho(k)|\langle\Phi_s^+|e\hat{D}|\Psi_s\rangle|^2, \quad \mathcal{F}_\downarrow = \rho(k)|\langle\Phi_s|e\hat{D}|\Psi_s\rangle|^2, \tag{25}$$

where $\rho(k)$ is the reduced density of states, $\hat{D}$ is the dipole moment operator, and e is the polarization vector of the light (where $|e_x|^2 + |e_y|^2 = 1$). Because Ψ_s and Φ_s are related to Ψ_s and Φ_s through Eq. (6), we have

$$\langle\Phi_s^-|e\hat{D}|\Psi_s\rangle = -\langle\Phi_s^+|e^*\hat{D}|\Psi_s\rangle^*.$$

Using the wave functions (13) and (24), we can obtain

$$|\langle\Phi_s^+|e\hat{D}|\Psi_s\rangle|^2 = {}^1/_2|NQ_+\mathcal{D}|^2|e_x(1-W_+) + ie_y(1+W_+)|^2, \tag{26}$$

where

$$\mathcal{D} = \langle S|\hat{D}_x|X\rangle, \tag{27}$$

$$|Q_+|^2 = \left|\frac{2(q_h^2-q_l^2)p_+}{(q_h^2-p_+^2)(q_l^2-p_+^2)}c_h\right|^2.$$

Analogously we can obtain

$$|\langle\Phi_s^-|e\hat{D}|\Psi_s\rangle|^2 = {}^1/_2|NQ_-\mathcal{D}|^2|e_x(1-W_-) - ie_y(1+W_-)|^2,$$

$$|Q_-|^2 = \left|\frac{2(q_h^2-q_l^2)p_-}{(q_h^2-p_-^2)(q_l^2-p_-^2)}s_h\eta\right|^2. \tag{28}$$

Using these relations, let us find an expression for the density matrix of the photoexcited electrons (at the instant of creation) for arbitrary polarization of the excitation beam incident along the z-axis:

$$\hat{\mathcal{F}}_0 = F_0\{\hat{I}[1+\alpha_0|e_x^2+e_y^2|\cos(2\psi)] + 2s_0\hat{\sigma}_z n_z\}, \tag{29}$$

where $\hat{\sigma}_z$ and $\hat{I}$ are the Pauli and unit matrix, $n_z = -i(e_x^* e_y - e_x e_y^*)$ is the angular momentum of the photon, and $\psi = \varphi_k - \varphi_e$ is the angle between the plane of preferred polarization of the light, where

$$\cos(2\varphi_e) = (|e_x|^2-|e_y|^2)/|e_x^2+e_y^2|,$$
$$\sin(2\varphi_e) = (e_x e_y^* + e_x^* e_y)/|e_x^2+e_y^2|,$$

and the vector connected with the direction k (in the spherical approximation it coincides with this direction). The parameters α_0 and s_0 determine the degree of alignment of the momenta and the average spin of the photoexcited electrons at the instant of creation for excitation by linearly polarized and circularly polarized light respectively. (For plane polarization $|e_x^2 + e_y^2| = 1$, $n_z = 0$, and for circular

polarization $|e_x^2 + e_y^2| = 1 = 0$, $n_z = \pm 1$.) For these values, and for F_0 as well, we obtain

$$\alpha_0 = -\frac{2W_\pm}{1+W_\pm^2}, \quad s_0 = -\frac{1}{2}\frac{1-W_\pm^2}{1+W_\pm^2},$$

$$F_0 = \frac{1}{2}|\mathcal{D}NQ_\pm|^2\rho(k)(1+W_\pm^2), \qquad (30)$$

where the upper sign refers to electron levels with odd index, and the lower sign to the levels with even index.

The main feature of Eq. (30) consists of the fact that in the spherical approximation, for which Eq. (20) is applicable, the quantities α_0 and s_0 depend only on the parameter $t = k^2/(k^2 + q_h^2)$, which can be interpreted as the squared sine of the angle of incidence of a heavy hole on the wall of the well.

In Figs. 1 and 2 we show the dependence of α_0 and s_0 on t corresponding to the two values of τ that are possible according to Eq. (15). These functions were calculated in the spherical approximation. Curves *1* on these figures correspond to the value τ_1 and refer to transitions between heavy-hole and electron levels with indices of the same parity or light-hole and electron levels with labels of different parity (for example, they refer to transitions $1hh$–$1e$,...,$2lh$–$1e$,...). Curves *2* correspond to values of τ_2 and refer to transitions between heavy-hole and electron levels with labels of different parity or to transitions between light-hole and electron levels with labels of the same parity (for example, to transitions $2hh$–$1e$,...,$1hh$–$2e$,...,$1lh$–$1e$,...). It is noteworthy that for different values of τ (curves *1*, *2*) the alignment values have opposite signs over the entire range of variation of t (Fig. 1) and orientations for $t < 2\nu/(3+\nu)$ (Fig. 2). For all the transitions, the alignment disappears as $k \to 0$ ($t \to 0$) and the orientation goes to its maximum possible value ($|s_0| \to 1/2$) but with opposite signs for curves *1* and *2*. For large values of k ($t \to 1$) the alignment reaches a maximum ($\alpha_0 \to 1$) for $\tau = \tau_1$ (curve *1*) and a small value of opposite sign ($\alpha_0 \to -6\nu/(9+\nu^2)$) for $\tau = \tau_2$ (curve *2*). In this case the orientation disappears for $\tau = \tau_1$ (curve *1*) and goes to a value close to its maximum ($s_0 \to -(9-\nu^2)/2(9+\nu^2)$) for $\tau = \tau_2$ (curve *2*). Let us note that for the transitions described by curves *2*, the alignment reaches a maximum value ($\alpha_0 = +1$) for $t = 2\nu/(3+\nu)$, and for this specific value of t the orientation passes through zero.

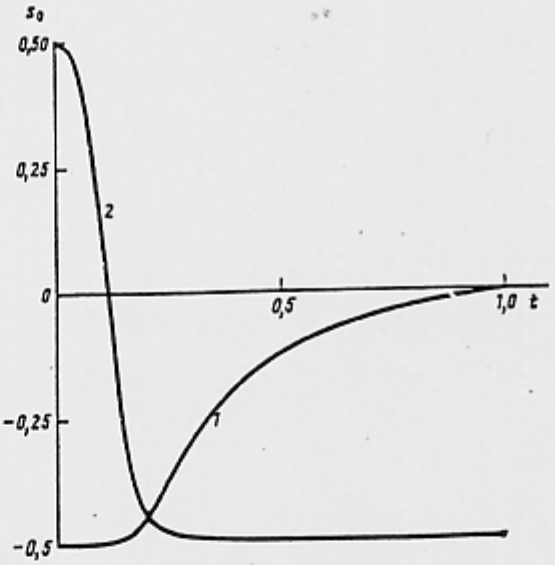

FIG. 2. Dependence of the average electron spin s_0 on t. The notation is the same as in Fig. 1.

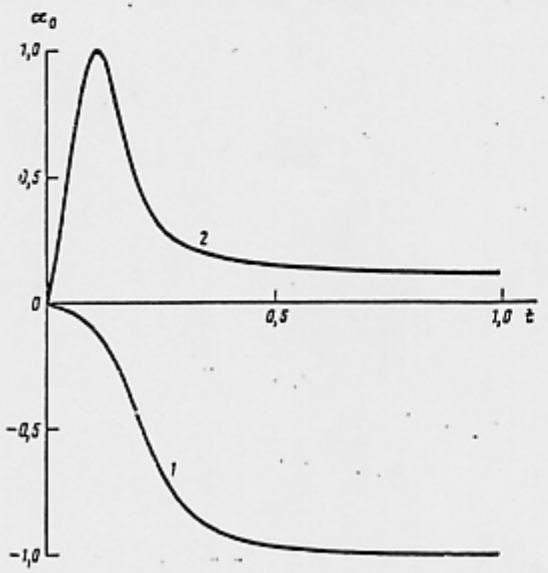

FIG. 1. Dependence of the alignment parameter α_0 on $t = k^2/(k^2 + q_h^2)$. We use the spherical approximation with $\nu = 0.18$. *1*—transition between heavy-hole levels and electron levels whose labels have the same parity, or transitions between light-hole levels and electron levels whose labels have different parity; *2*—remaining transitions.

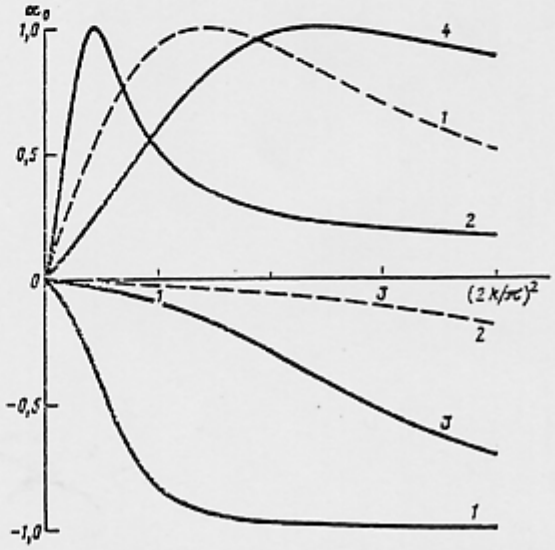

FIG. 3. Dependence of the alignment parameter α_0 on k^2 for electrons photoexcited to the first size-quantized level. The half-width of the well is taken to be the unit of length. We use the spherical approximation with $\nu = 0.18$. The solid curves are transitions from the heavy-hole subbands, the dashed are from the light-hole subbands. The numbers on the curves label the hole subbands.

There is some practical interest in the k-dependence of the degrees of orientation and alignment. In order to obtain these dependences by using Figs. 1 and 2 we require a relation between the parameter t and the wave vector k. We can obtain this relation from Eqs. (11), (15), and (19). The resulting functions are shown in Figs. 3 and 4 for transitions to the first electron level. Figure 5 shows the k-dependence of the total rate of generation F_0 of electrons calculated by using the last of Eqs. (30). Figure 6 shows the spectrum of holes in the size-quantized bands. All the curves on Figs. 1–6 were calculated for a value of $\nu = m_l/m_h = 0.18$.[2)]

6. We note that all the characteristics of these transitions undergo an abrupt change for small values of $k \approx \nu^{1/2}/L$. This is related to the abrupt reconstruction of the wave function for holes that was mentioned in Sec. 4 for $t \approx 4\nu/3$. This behavior of the wave function is caused by a virtual surface state—which becomes real for $\nu < 0$ (see Ref. 11)—that affects the reflection of holes from the walls of the well (see also Ref. 12). For this reason, when $\nu \ll 1$ the behavior of the alignment and orientation in a quantum well exhibits a paradoxical departure from the sort of behavior that analogies with the three-dimensional case would predict.

In the three-dimensional case, when the excitation beam is parallel to the z-axis and polarized along the x-axis the angular dependence of the distribution function of electrons photoexcited from the heavy-hole band has the form[1-3] $\mathcal{F} \propto (k_y^2 + k_z^2)$. This is because the selection rules forbid the excitation of electrons with k directed along x in this case. Expressing this function in terms of the angle φ_k which the two-dimensional vector (k_x, k_y) makes with the x-axis, by analogy with Eq. (29) we obtain $\alpha_0 = -k^2/(k^2 + 2k_z^2)$, where $k^2 = k_x^2 + k_y^2$. It would be natural to assume that k_z can be identified with the value π/L, which is a quantity on the order of the z-component of the momentum in the first size-quantized subband of an electron; this formula should then give a correct description of the k-dependence of α_0 for this subband. These simple considerations were in fact used to estimate the degree of alignment in Ref. 7, resulting in a correct description of the overall form of the function $\alpha_0(k)$, i.e., zero alignment as $k \to 0$ and complete alignment as $k \to \infty$. However, $\alpha_0(k)$ does not contain any dependence on ν and predicts a smooth increase of $|\alpha_0|$ from zero up to unity as k increases. However, the calculations we have presented above indicate that for $\nu \ll 1$ the alignment increases rapidly to its maximum value even when $kL \approx \nu^{1/2}$.

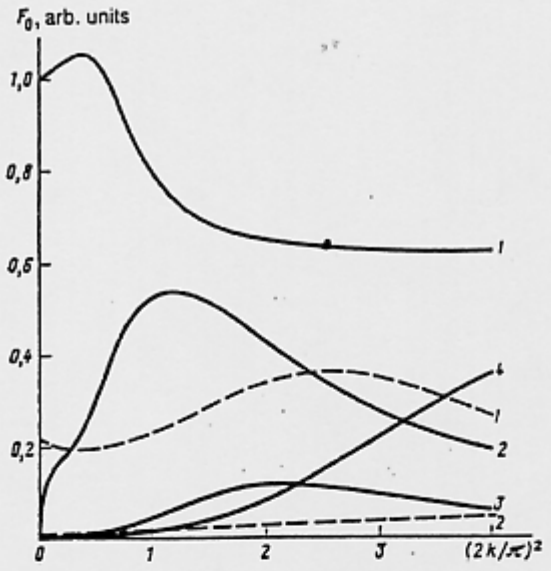

FIG. 5. Dependence of the generation rate F_0 for electrons to the first size-quantized level on k^2. The notation is the same as in Fig. 3.

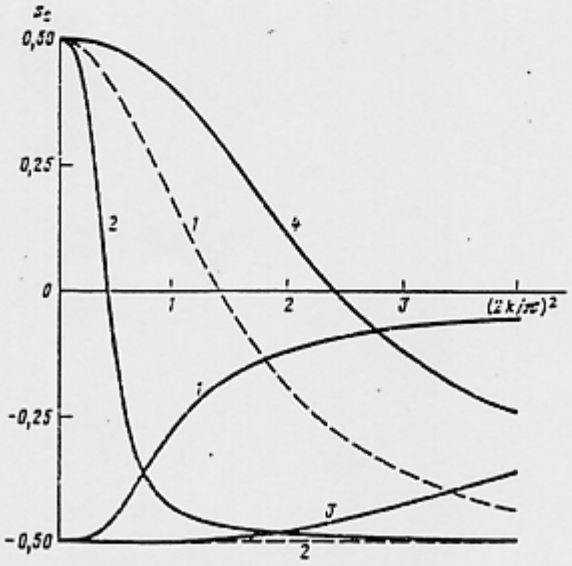

FIG. 4. Dependence of the average spin s_0 on k^2 for electrons photoexcited to the first size-quantized level. The notation is the same as in Fig. 3.

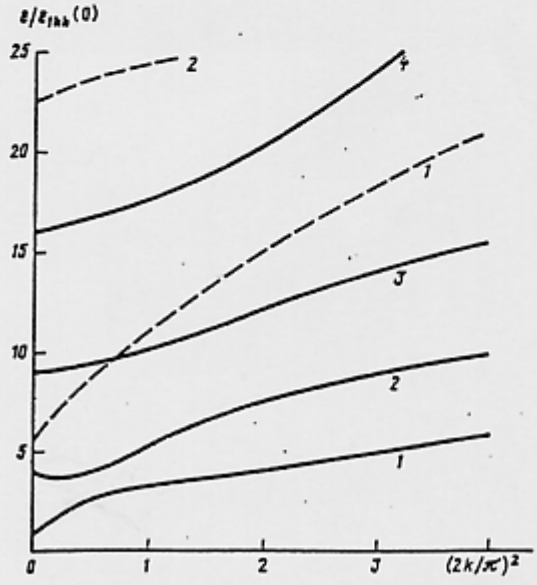

FIG. 6. Spectrum of holes in the size-quantized bands. We use the spherical approximation with $\nu = 0.18$. The solid curves are heavy holes, the dashed curves are light holes. The labels on the curves correspond to labels of the subbands.

7. Orientation and alignment of electrons are usually detected by looking for circular and linear polarization of the recombination radiation. The intensity J_{e_1} of radiation with polarization e_1 is given by the formula

$$J_{e_1}=C\int_0^{2\pi}d\varphi_k\sum_{mm'}\mathcal{F}_{mm'}\left(\sum_{\mu}\langle\Phi_{m'}|e_1\hat{D}|f_\mu\rangle\langle\Phi_m|e_1\hat{D}|f_\mu\rangle^*\right), \tag{31}$$

where C is a function of the frequency of light and is determined by the reduced density of states and the number of holes for the state f_μ (μ is an index that enumerates the degenerate states of the holes; we assume that the holes are neither aligned nor oriented). $\mathcal{F}_{mm'}$ is the density matrix of the recombining electrons (which in the present case is diagonal), and is determined by using expressions that differ from (29) only by the replacement of α_0 and s_0 by α and s, taking into account the relaxation processes. When the recombination radiation propagates along the z-axis, the matrix of observation (with respect to the indices mm') whose elements are contained in the circular brackets of Eq. (31) is also analogous to Eq. (29). This matrix differs from (29) only by the replacement of the parameters α_0 and s_0 by α_1 and s_1, which depend on the final states of the recombining electrons. From Eq. (31) it follows that for linearly polarized excitations the recombination luminescence will also be linearly polarized; the degree of polarization (with respect to the polarization of the excitation) is determined by the expression

$$P_l={}^1/_2\alpha_1\alpha. \tag{32}$$

For a circularly polarized pump the radiation will have a circular polarization P_c, where

$$P_c=4ss_1. \tag{33}$$

If free holes belonging to one of the size-quantized levels participate in the recombination, then $s_1(\mathbf{k})=s_0(\mathbf{k})$, $\alpha_1(\mathbf{k})=\alpha_0(\mathbf{k})$. In this case $\alpha_0(\mathbf{k})$ and $s_0(\mathbf{k})$ should be calculated for transitions between subbands that participate in the recombination luminescence. Figure 7 shows the dependence of the degrees of polarization P_l and P_c for radiation emitted during the recombination of electrons excited in $1hh$–$1e$ transitions with nonoriented and nonaligned holes in levels $1hh$ (the process $1hh$–$1e$–$1hh$). The calculation is shown for luminescence quantum energies that are close to the energies of the excitation quanta, so that relaxation processes are unimportant ($\alpha=\alpha_0$, $s=s_0$). Let us recall that the signs of the parameters α can be opposite for excitation and recombination (e.g., for the process $1lh$–$1e$–$1hh$). In this case P_l will be negative. The same applies for P_c as well.

8. Let us now discuss the role of cubic (not spherical) symmetry of the crystal. As is well known,[1-3] in the three-dimensional case this leads to a dependence of the degree of linear polarization of the hot luminescence on the orientation of the plane of polarization of the excitation with respect to the crystallographic axes. An analogous effect also occurs in quantum wells. For its description we will use an approximation analogous to that used in Ref. 1 for the three-dimensional case. That is, we will assume that the primary contribution to the recombination radiation comes from carriers

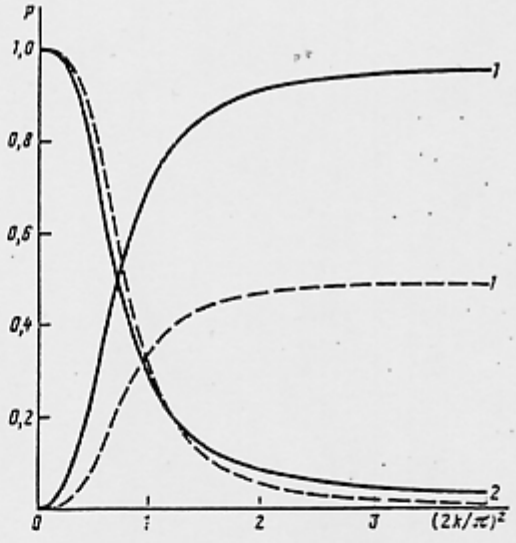

FIG. 7. Dependence of the linear (P_l) and circular (P_c) polarizations of the luminescence on k^2 for the process $1hh$–$1e$–$1hh$. The dashed curves are the spherical approximation, $\nu=0.18$. The solid curves are the diagonal approximation with $\gamma_1=6.79$, $\gamma_2=1.924$, $\gamma_3=2.681$ (GaAs, Ref. 13). 1—P_l, $P_{l\max}$, 2—P_c.

for which the wave vector k points in the direction that minimizes the energy of the holes for a given value of k. This approximation is correct for hot luminescence at low temperatures when the number of holes that participate in the recombination decreases rapidly with increasing energy. In the three-dimensional case this direction coincides with the direction $\{111\}$. For the case under discussion here, i.e., quantum wells parallel to the plane (001), the corresponding direction of the two-dimensional vector k is along one of the two axes [110] and [$1\bar{1}0$] (see, e.g., Ref. 5).

For recombination of holes on an acceptor we also may assume that this direction plays a fundamental role (in analogy with the three-dimensional case[1-14]). In this diagonal approximation, if the polarization vector e of the excitation light is parallel to the [100] or [010] axis, then linear polarization of the luminescence is absent ($P_l=0$), since the occupations of the directions [110] and [$1\bar{1}0$] are the same in this case from symmetry considerations. We should expect the maximum polarization of the luminescence when the vector e is parallel to one of the directions [110] or [$1\bar{1}0$]. For the process $1hh$–$1e$–$1hh$ at the short-wavelength edge of the hot-luminescence spectrum we find that $P_{l\max}=\alpha_0^2$, where α_0 should be determined from the first of Eqs. (30) by calculating W_+ from (14) and (3) for $k_x^2=k_y^2=k^2/2$. In Fig. 7 the solid curves give values of $P_{l\max}$ and P_c calculated in this way for the process $1hh$–$1e$–$1hh$ (P_c was calculated using Eqs. (33) and (30) under the assumption that $s_1=s=s_0$ with the same values of W_+). Let us note that for these processes $P_{l\max}+P_c=1$ holds in the diagonal approximation, while $2P_l+P_c=1$ holds in the spherical approximation.

9. The linear and circular polarization of hot photoluminescence from quantum wells was investigated in Refs. 7 and 15.[3)] The observed dependence of P_l and P_c on energy of the exciting photons $\hbar\omega_{exc}$ agrees qualitatively with the calculations described above. Specifically, P_l increases with in-

creasing $\hbar\omega_{exc}$ while P_c decreases. These authors also observed a strong anisotropy in the linear polarization. The maximum value of P_l corresponds to polarization of the excitation along the [110]-axis. However, there is a significant quantitative disagreement between theory and experiment: the linear polarization in the experiment is very much smaller, while the circular is very much larger, than is predicted by theory. Furthermore, the experimental dependence of P_l and P_c on $\hbar\omega_{exc}$ is found to be too smooth. These disagreements are possibly related to the fact that in the experiments the observed radiation is due to band-to-acceptor rather than band-to-band recombination, as was assumed above. In addition, the finiteness of the depth of the quantum well may affect the result, as well as strain in the gallium arsenide layer of the heterostructure.

The authors are grateful to M. I. D'yakonov and D. N. Mirlin for discussions of the results and stimulating comments, and also to P. L. Roskin for his assistance in the calculations.

[1)] This circumstance was called to our attention by A. V. Subashiev and L. G. Gerchikov.

[2)] This value corresponds to the spherical approximation for GaAs. The spherical approximation is apparently a poor description with regard to finding the location of the levels for $k = 0$.[9] However, it is useful for clarifying the general regularities in the behavior of orientation and alignment.

[3)] In this paper we will not touch on experimental and theoretical investigations of the polarization characteristics of luminescence that propagates in the plane of the well (see, e.g., Refs. 16 and 17). In this case the polarization of the luminescence is due not to the polarization of the excitation but to the presence of a preferred axis, i.e., the normal to the plane of the heterostructure (see also Ref. 18).

[1] B. P. Zakharchenya, D. N. Mirlin, V. I. Perel', and I. I. Reshina, Usp. Fiz. Nauk 136, 459 (1982) [Sov. Phys. Usp. 25, 143 (1982)].
[2] M. A. Alekseev, I. Y. Karlik, D. I. Mirlin, and V. F. Sapega, Fiz. Tekh. Poluprovodn. 23, 761 (1989) [Sov. Phys. Semicond. 23, 479 (1989)].
[3] *Optical Orientation*, F. Meier and B. P. Zakharchenya eds., North-Holland, Amsterdam, 1984 (Translation: *Opticheskaya orientatsiya*, Nauka, Leningrad, 1989).
[4] E. L. Ivchenko, P. S. Kop'ev, V. P. Kochereshko *et al.*, Pis'ma Zh. Eksp. Teor. Fiz. 47, 407 (1988) [JETP Lett. 47, 486 (1988)].
[5] C. Weisbuch, *Applications of Multiquantum Wells, Selective Doping, and Superlattices* (Series *Semiconductors and Semimetals*, R. Dingle ed., Vol. 24, p. 46, Academic, London, 1987).
[6] A. Twardowski and C. Hermann, Phys. Rev. B 35, 8144 (1987).
[7] B. P. Zakharchenya, P. S. Kop'ev, D. N. Mirlin *et al.*, Solid State Commun. 69, 203 (1989).
[8] Y. C. Chang and I. N. Schulman, Phys. Rev. B 31, 2069 (1985).
[9] E. I. Rashba and E. Ya. Scherman, Phys. Lett. A 129, 175 (1988).
[10] S. S. Nedorezov, Fiz. Tverd. Tela (Leningrad) 12, 2269 (1970) [Sov. Phys. Solid State 12, 1814 (1970)].
[11] M. I. D'yakonov and A. V. Khaetskii, Zh. Eksp. Teor. Fiz. 82, 1584 (1982) [Sov. Phys. JETP 55, 917 (1982)].
[12] L. G. Gerchikov, and A. V. Subashiev, Phys. Status Solidi (b) 160, 443 (1990).
[13] L. W. Molenkamp, R. Eppenga, G. W. t'Hooft *et al.*, Phys. Rev. B 38, 4314 (1988).
[14] M. A. Alekseev, I. Y. Karlik, I. A. Merkulov *et al.*, Fiz. Tverd. Tela (Leningrad) 27, 2650 (1985) [Sov. Phys. Solid State 27, 1589 (1985)].
[15] P. S. Kop'ev, D. I. Mirlin, D. G. Polyakov *et al.*, Fiz. Tekh. Poluprovodn. 24, 1200 (1990) [Sov. Phys. Semicond. 24, 757 (1990)].
[16] R. Sooryakumar, IEEE J. Quantum Electron. QE-22, 1645 (1986).
[17] S. Colak, R. Eppenga, and M. F. H. Schuurmans, IEEE J. Quantum Electron. QE-23, 960 (1987).
[18] F. T. Vas'ko and G. I. Steblovskii, Fiz. Tekh. Poluprovodn. 24, 59 (1990) [Sov. Phys. Semicond. 24, 36 (1990)].

Translated by Frank J. Crowne